CIRP Annals - Manufacturing Technology 67 (2018) 181–184

Contents lists available at ScienceDirect

CIRP Annals - Manufacturing Technology

journal homepage: http://ees.elsevier.com/cirp/default.asp

Nanoscale surface patterning of diamond utilizing carbon diffusion reaction with a microstructured titanium mold

Jiwang Yan (2)*, Yuji Imoto

Department of Mechanical Engineering, Keio University, Yokohama 223-8522, Japan

ARTICLE INFO

Article history:
Available online 26 April 2018

Keywords:
Diamond
Nanostructure
Surface integrity

ABSTRACT

A novel method was proposed for generating nanoscale surface patterns on single-crystal diamond by carbon diffusion with a microstructured titanium mold under controlled temperature and pressure. The depth, geometry, and surface integrity of the fabricated patterns were investigated by laser micro-Raman spectroscopy and white-light interferometry, and the titanium molds were analyzed by energy dispersive X-ray spectroscopy. The results showed that at specific temperatures and pressures, three-dimensional patterns with a depth of tens of nanometers and sloped/curved walls could be generated on a diamond surface after a few minutes, without causing any surface graphitization. The intensity profile and penetration depth of carbon atoms into the titanium were experimentally measured.

1. Introduction

Single-crystal diamond has excellent material properties such as high hardness, thermal conductivity, electrical resistance, and chemical stability, thus it is an important substrate material for cutting tools, power electronics, micro electrical mechanical systems, etc. [1]. There is an increasing demand in industry for the fabrication of large-area micro/nanoscale surface patterns at high precision and low cost. However, due to the high hardness, it is extremely difficult to machine diamond by mechanical methods. Electrical machining can be used to machine sintered poly-crystal diamond [2], but cannot be used for single-crystal diamond due to its insulation properties. Focused ion beam technology can be used to machine diamond, but it is extremely expensive and time- consuming when machining large-area surfaces. Ultra-short pulsed laser has been attempted for machining diamond [3,4], but the surface quality is still low with considerable subsurface damage. In addition, for all the above-mentioned methods, it is difficult to control machining depth at nanometer resolution. In this study, a novel method is proposed to generate nanoscale surface patterns on diamond based on the carbon diffusion reaction with a microstructured titanium mold under controlled temperature and pressure. The resulting depth, geometry, and surface integrity of the patterns were investigated under various conditions. 3D patterns were rapidly fabricated without surface graphitization.

2. Mechanism for pattern generation

Though diamond is stable at room temperature, it has high affinity with specific transition metals at a high temperature [5]. Carbon atoms in diamond will diffuse into the transition metals through their contact interface, causing gradual removal of diamond from the surface. As a result, intensive wear occurs to diamond tools when cutting these metals [6–8]. On the other hand, by utilizing the carbon diffusion reaction, a few thermochemical methods have been developed for machining diamond [9–11]. Nevertheless, for ferrous metals Cr, Fe, Co and Ni, catalytic graphitization of diamond occurs before the diffusion reaction [10–12], which causes surface roughening and surface integrity degradation.

In this study, Ti is proposed as a mold material for machining of diamond. Ti is a VI-family metal having 2 *d* electrons. Fig. 1 shows various transition metals plotted with respect to *d* electron number and melting point. Zr, Ta, W, Nb, Mo and Cu have low affinity with diamond due to their high activation energy for carbon diffusion. For other metals, the number of *d* electrons affects the affinity with diamond [13]. Cr, Fe, Co and Ni have 5–8 *d* electrons, thus their affinity with diamond is low. However, their catalytic effect is so strong that upon contact, diamond transforms immediately to graphite before carbon diffusion occurs (Fig. 2(a)). In contrast, Ti and V can react with diamond directly, forming carbides. Ti can absorb carbon atoms from a diamond surface without inducing graphitization (Fig. 2(b)). This unique feature of Ti enables machining of diamond without surface roughening and

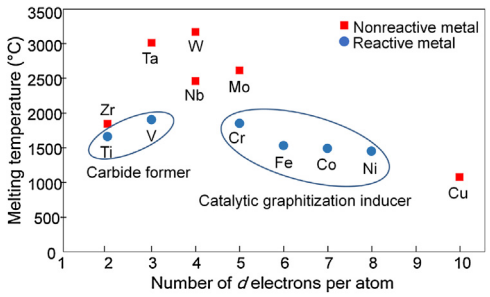

Fig. 1. Reactivity with diamond for various transition metals.

* Corresponding author.
E-mail address: yan@mech.keio.ac.jp (J. Yan).

https://doi.org/10.1016/j.cirp.2018.04.067
0007-8506/

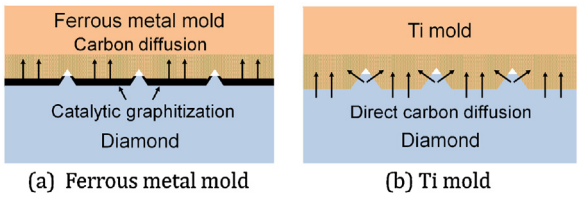

Fig. 2. Surface patterning mechanisms of diamond.

graphite residue. When a structured Ti mold is pressed against diamond under high temperature and pressure, carbon atoms are directly absorbed by the Ti. In this way, localized removal of diamond can be realized without leaving a graphite layer. This thermochemical machining method enables the generation of large-area surface patterns by one-step press molding, which provides high productivity, like the nanoimprinting technology.

3. Experimental procedures

Single-crystal diamond blocks ($3.0 \times 3.0 \times 1.5\ mm^3$) having (100) surface planes with a mirror finish (surface roughness 1.2 nmSa) were used as the specimens. A nanoindentation system was used to create micro dimples on flat Ti molds having 6 mm diameter, 2 mm thickness, and 10 nmRa surface roughness. Fig. 3 shows SEM photographs of dimples indented on Ti molds by using a Berkovich indenter and a conical indenter. A high-precision molding machine GMP211 (Toshiba Machine Co. Ltd., Japan) was used for the pressing tests, which enables multi-workpiece pressing over an area of 80 mm diameter. Heating was realized by infrared lamps, and temperature was controlled in the range of 600–800 °C with ±1 °C accuracy. Pressing force was controlled with a resolution of 0.98 N to control pressure (~60 MPa). The molding chamber was covered by a quartz tube purged with Ar gas. To prevent stress concentration, 2 mm-thick elastic ceramic sheets were used to cover the diamond sample and the mold from two sides. The patterns formed on the diamond surface were observed using a field emission scanning electron microscope (FE-SEM) (Sirion, FEI Co., USA). The material composition of the mold surface was detected by an energy dispersive X-ray spectroscope (EDS) (XFlash Detector 4010, Bruker Co., Germany). The crystalline structure of the patterns on diamond was characterized by a laser micro-Raman spectroscope (NRS-3100, JASCO Co., Japan). The pattern depth and surface topographies were measured using a white-light interferometer (CCI3D, Taylor Hobson Co., Ltd., UK).

4. Results and discussion

4.1. Pattern geometry and surface integrity

Fig. 4(a)is a micrograph of patterns generated on diamond at 800 °C and 30 MPa after a pressing time of 15 min. Triangular patterns were clearly replicated from the pyramidal dimples on the Ti mold (Fig. 3(a)). There was no black graphite residue on the surface after pressing. Fig. 4(b) shows Raman spectra of machined and unmachined surface areas. Both spectra show sharp peaks at 1332 cm^{-1}, indicating a structure of single-crystalline diamond without phase transformation. Fig. 5 shows SEM photographs of the patterns at different magnifications. The protruding regions are very smooth (1.2 nmSa), indicating that these regions were unaffected by pressing; whereas the surrounding region is rougher (5.9 nmSa) due to chemical reaction with Ti. Fig. 6 shows a 3D topography and a cross-sectional profile of the patterns. The average height of the protrusions is ~40 nm.

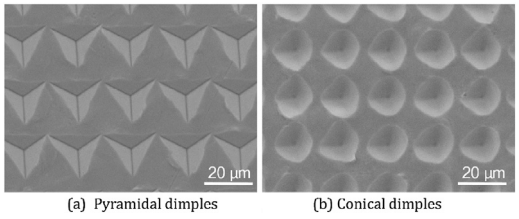

Fig. 3. SEM photographs of micro dimples indented on Ti mold surfaces.

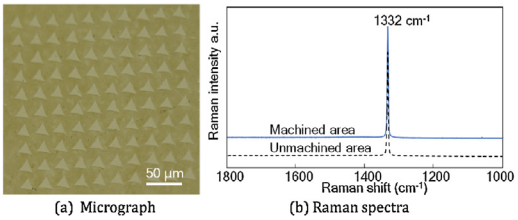

Fig. 4. Micrograph and Raman spectra of patterns generated on diamond.

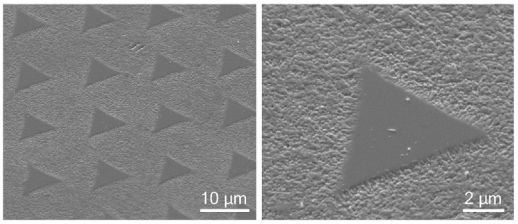

Fig. 5. SEM photographs of patterns generated on diamond surface.

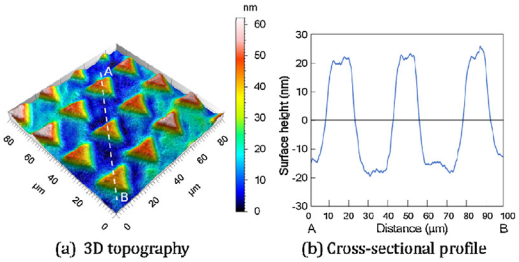

Fig. 6. 3D topography and cross-sectional profile of patterns in Fig. 5.

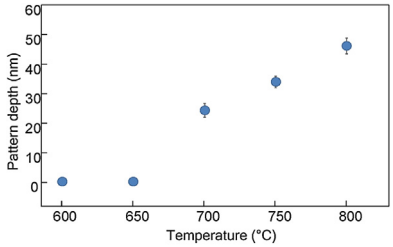

Fig. 7. Change of pattern depth with temperature.

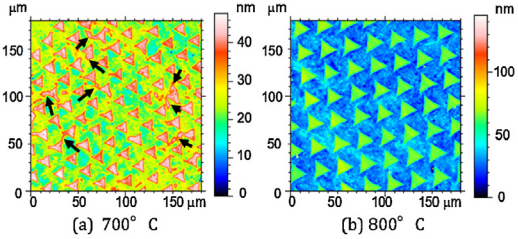

Fig. 8. Effect of temperature on pattern profile integrity.

4.2. Effect of temperature

Pressing tests (15 min each) were performed at temperatures ranging from 600 °C to 800 °C at intervals of 50 °C while the pressure

was fixed at 30 MPa. The change in pattern depth with temperature is shown in Fig. 7. Below 650 °C, pattern depth is zero, indicating that no carbon diffusion occurs. As the temperature increases from 700 °C to 800 °C, the pattern depth increases from 24 nm to 46 nm proportionally, indicating the possibility of controlling pattern depth at a nanometer level by changing the temperature.

Fig. 8 shows patterns generated at different temperatures. At 700 °C, there are some incompletely replicated regions as indicated by arrows in Fig. 8(a), illustrating that the carbon diffusion rate is not uniformly distributed. In contrast, all the patterns were uniformly replicated at 800 °C (Fig. 8(b)). This result displays that a higher temperature helps to improve pattern profile integrity.

4.3. Effect of pressure

Pressing tests were performed at a higher pressure of 60 MPa at different temperatures. The resulting surface patterns are shown in Fig. 9. At 60 MPa and 700 °C, all the patterns were uniformly replicated without the irregular regions observed at 30 MPa and 700 °C as shown in Fig. 8(a). This indicates that increasing pressure can improve the uniformity of interfacial contact and the carbon diffusion rate between diamond and Ti. A high pressure is especially important for improving the pattern profile integrity when a low pressing temperature is used. On the other hand, even when the pressure was changed from 30 MPa to 60 MPa, no significant change was found in pattern depth. This indicates that although pressure can improve the uniformity of interfacial contact and carbon diffusion rate, it does not dramatically change the total amount of carbon diffusion from diamond to Ti.

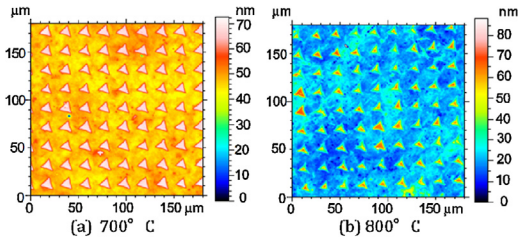

Fig. 9. Topographical change of surface patterns at a high pressure of 60 MPa and different temperatures.

At 60 MPa and 800 °C, patterns were also uniformly replicated (Fig. 9(b)). However, distinctly different from Fig. 9(a) where the protrusions have flat tops, the protrusions in Fig. 9(b) have pointed tops and sloped side walls. Fig. 10(a)is an enlarged view of the patterns in Fig. 9(b). A gradient can be clearly identified within each protruding region, indicating a change in local surface height. Each protrusion is akin to a pyramid, which is similar to the shape of the Berkovich indenter used for generating dimples on the Ti mold. Fig. 10(b) is a cross-sectional profile of a protrusion. The height of the protrusion is ~40 nm. The angles of the right and left sides, which correspond to a face and a ridge of the Berkovich indenter, respectively, are different.

Similar results were observed for experiments using a conically dimpled Ti mold. Fig. 11(a) and (b) shows 3D topographies of surface patterns generated using a conically dimpled Ti mold at the same temperature of 800 °C but at different pressures: 30 MPa and 60 MPa, respectively. The pressing time was 15 min. It is evident that the protrusions in Fig. 11(a) have flat tops, whereas those in Fig. 11(b) have conical shapes. Fig. 12(a) and (b) are cross-sectional profiles of the protrusions measured along the lines AB and CD, respectively, in Fig. 11. The profiles confirm again that the protrusions formed at 30 MPa are flat-topped, whereas those generated at 60 MPa are nearly conical. The change of protrusion shape might be due to the pressure-induced elastic deformation of mold material around a dimple. Generating such protrusions with curved/sloped profiles on diamond might provide a new approach to 3D surface patterning of diamond. These patterns are useful for texturing diamond cutting

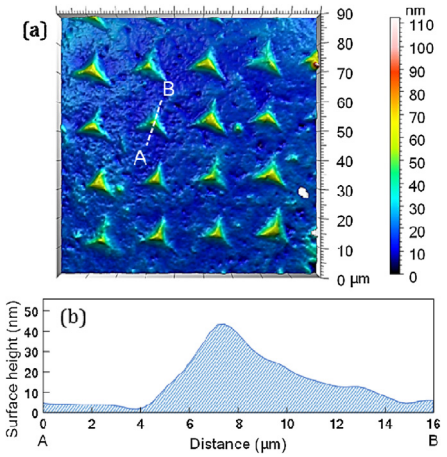

Fig. 10. Topography and cross-sectional profile of surface protrusions generated at 60 MPa and 800 °C, showing pointed tops and sloped walls.

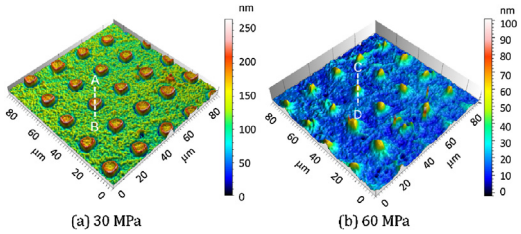

Fig. 11. 3D topographies of surface protrusions generated using a conically dimpled Ti mold at different pressures.

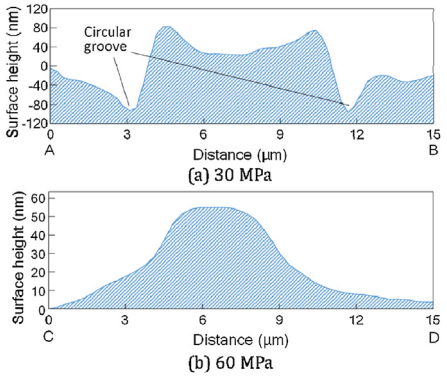

Fig. 12. Cross-sectional profiles of surface protrusions generated using conical dimples at different pressures.

tools, diamond slider heads, and other functional components of diamond. In addition, a circular groove can be observed around the protrusion at 30 MPa (Fig. 12(a)), which is replicated from the burrs around the dimples generated during indentation. At 60 MPa, however, the burrs were flattened during pressing, and no groove is observed around the protrusion (Fig. 12(b)).

4.4. Effect of pressing time

To investigate the effect of pressing time on pattern depth and topography, experiments were performed for various lengths of time at 30 MPa and 800 °C. It was found that the depth of patterns increased slightly with the pressing time, but the change was insignificant. For example, the pattern depth after 5 min pressing was 41 ± 5 nm, and that after 15 min pressing was 46 ± 3 nm. This result means that surface patterns with a depth of tens of nanometers can be rapidly generated within a few minutes, demonstrating a high productivity for the proposed method. An excessively long time will not distinctly increase the pattern depth due to the saturation of carbon in the surface layer of the Ti mold. The saturated layer is extremely thin and can be easily removed by polishing and/or acid etching for the reuse of the mold.

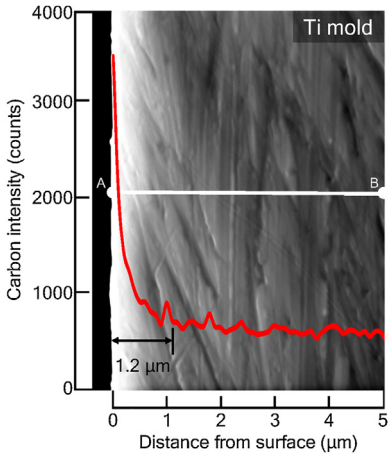

Fig. 13. Cross-sectional EDS analysis of carbon intensity profile in Ti mold after pressing diamond.

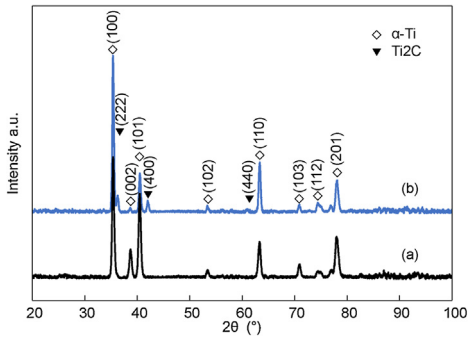

Fig. 14. XRD spectra of Ti mold surface before/after pressing diamond.

4.5. Interfacial carbon diffusion analysis

To confirm the carbon diffusion phenomenon, EDS analysis was performed on the Ti mold after the experiments. Fig. 13 shows a cross-sectional EDS analysis of the carbon intensity profile in a Ti mold after pressing diamond at 30 MPa and 800 °C for 15 min. This intensity profile was obtained along the line AB in the figure. It is evident that the carbon intensity at the surface contacting the diamond is quite high, and this intensity decreases with the depth from the surface. The penetration depth of carbon into Ti reaches 1.2 μm. This result verifies the pattern formation mechanism in Fig. 2(b), namely, intensive carbon diffusion from diamond into Ti leads to local material removal from the diamond.

Fig. 14 illustrates XRD spectra of a Ti mold surface before and after pressing diamond. As indicated by spectrum (a), before pressing, peaks are detected at (100), (002), (101), (102), (110), (103), (112), and (201), which are typical peaks for the crystal planes of α-Ti. After pressing diamond, as shown by spectrum (b), apart from the α-Ti peaks, new peaks are detected at (222), (400) and (440), indicating the crystal planes of Ti_2C. This result demonstrates that carbon atoms diffused from diamond have combined with Ti atoms, forming Ti_2C. This phenomenon is similar to that which occurs in Ti coating on diamond [14].

Finally, topographies of the contacting surfaces of both Ti and diamond were examined after pressing at 30 MPa and 800 °C for 15 min. Dot marking was used to identify the corresponding locations of the contacting areas for both materials, as shown in Fig. 15(a) and (b) . As seen in Fig. 15(a), the Ti surface became uneven due to carbon diffusion and grain coarsening, whereas the diamond surface remained flat (Fig. 15(b)). Fig. 15(c) shows cross-sectional profiles measured along the lines AB and A'B' in Fig. 15(a) and (b). A grain boundary step of ~100 nm occurred on the Ti surface, but the diamond surface has a peak-to-valley distance of ~15 nm. This result indicates that even though Ti undergoes

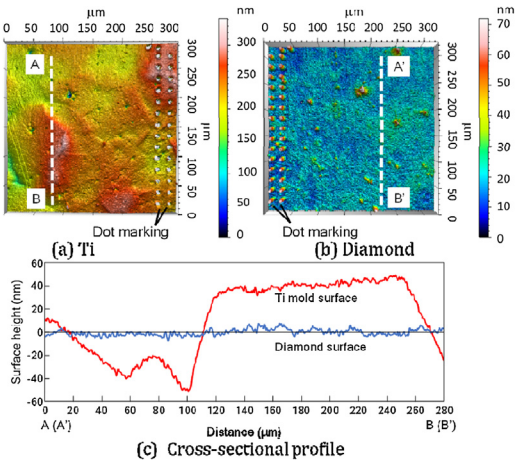

Fig. 15. Topographies of contact surfaces of (a) Ti and (b) diamond after pressing. (c) is a comparison of their cross-sectional profiles.

recrystallization and the mold surface becomes bumpy, it is pressed flat by the diamond at high pressure, resulting in a uniform carbon diffusion rate.

5. Conclusions

Fine patterns with a depth of tens of nanometers were generated on single-crystal diamond via carbon diffusion reaction with micro-dimpled Ti molds under controlled temperature and pressure. The pattern depth was strongly dependent on the temperature and less affected by pressure. The cross-sectional shape of patterns changed greatly with pressure. Patterns with sloped/curved walls were obtained at a high pressure. The pattern has a single-crystalline structure without graphitization. Pattern generation could be completed within a few minutes, demonstrating high productivity for large-area functional surfaces on diamond.

References

[1] Schreck M, Asmussen J, Shikata S, Arnault JC, Fujimori N (2014) Large-area High-quality Single Crystal Diamond. *MRS Bulletin* 39(6):504–510.
[2] Yan J, Watanabe K, Aoyama T (2014) Micro-electrical Discharge Machining of Polycrystalline Diamond Using Rotary Cupronickel Electrode. *CIRP Annals — Manufacturing Technology* 63(1):209–212.
[3] Kim J, Je TJ, Cho SH, Jeon EC, Whang KH (2014) Micro-cutting with Diamond Tool Micro-patterned by Femtosecond Laser. *International Journal of Precision Engineering and Manufacturing* 15(6):1081–1085.
[4] Takayama N, Yan J (2017) Laser Irradiation Responses of a Single-Crystal Diamond Produced by Different Crystal Growth Methods. *Applied Sciences* 7 (8):815.
[5] Tanaka T, Ikawa N, Tsuwa H (1981) Affinity of Diamond for Metals. *CIRP Annals — Manufacturing Technology* 30(1):241–245.
[6] Hartung PD, Kramer BM, Turkovich BF (1982) Tool Wear in Titanium Machining. *CIRP Annals — Manufacturing Technology* 31(1):75–80.
[7] Paul E, Evans CJ, Mangamelli A, Mcglauflin ML, Polvanit RS (1996) Chemical Aspects of Tool Wear in Single Point Diamond Turning. *Precision Engineering* 18:4–19.
[8] Shimada S, Tanaka H, Higuchi M, Yamaguchi T, Obata K (2004) Thermo-Chemical Wear Mechanism of Diamond Tool in Machining of Ferrous Metals. *CIRP Annals — Manufacturing Technology* 53(1):57–60.
[9] Mehedi H, Hebert C, Ruffinatto S, Eon D, Omnes F, Gheeraert E (2012) Formation of Oriented Nanostructures in Diamond Using Metallic Nanoparticles. *Nanotechnology* 23455302.
[10] Wang J, Wan L, Chen J, Yan J (2015) Anisotropy of Synthetic Diamond in Catalytic Etching Using Iron Powder. *Applied Surface Science* 346:388–393.
[11] Imoto Y, Yan J (2017) Thermochemical Micro Imprinting of Single-crystal Diamond Surface Using a Nickel Mold under High-pressure Conditions. *Applied Surface Science* 404:318–325.
[12] Uemura M (2004) An Analysis of the Catalysis of Fe, Ni or Co on the Wear of Diamonds. *Tribology International* 37:887–892.
[13] Artini C, Muolo ML, Passerone A (2012) Diamond-metal Interfaces in Cutting Tools: A Review. *Journal of Material Science* 47(7):3252–3264.
[14] Zhu Y, Zheng B, Yao W, Cao L (1999) The Interface Diffusion and Chemical Reaction Between a Ti Layer and a Diamond Substrate. *Diamond and Related Material* 8:1073–1078.